

NON-DESTRUCTIVE TESTING USING TWO-COMPONENT/TWO-WAVE MIXING INTERFEROMETER

A. Wartelle, B. Pouet, and S. Breugnot

Bossa Nova Technologies, Venice, CA 90291

ABSTRACT. A new laser-based ultrasonic (LBU) receiver was recently introduced. The novel architecture is based on two-wave mixing in photorefractive materials and allows simultaneous measurement of in-plane and out-of-plane displacements (two-component). By taking advantage of recent developments in electronic processing and our knowledge on multi-channel interferometer, we achieved a compact optical system using only a single collecting aperture and a single laser probe beam. We will characterize the system performances and present experimental results demonstrating the capability for this compact two-component interferometer.

Keywords: Speckles, Ultrasound, Ultrasonic Testing, Interferometry Holographic, Lasers

PACS: 42.30.Ms; *43.35.-c; 43.35.+d, 81.70.Cv; 42.40.Kw; 42.55.-f

INTRODUCTION

Laser-based ultrasonic (LBU) is now becoming a more mature technology. The main well-known advantages of LBU are its ability to perform remote / non-contact measurements, as well as its point-like and broadband detection. To date, LBU inspection systems are still mostly based on the confocal Fabry-Pérot interferometer [1, 2] or Two Wave Mixing interferometer in photorefractive crystal [3]. These systems only measure the surface displacement along the direction of observation (the out-of-plane displacement for observation normal to the surface). Modifications of these systems were previously demonstrated for detection of two components [4], but they stayed limited to laboratory demonstration. To date, only low frequency (<1MHz) systems are commercially available for measuring simultaneously multi-component [5].

We recently proposed a new interferometric receiver for high sensitivity and simultaneous detection multi-component detection. This interferometer is based on a two-wave mixing interferometer designed for high sensitivity measurements in laboratories on optically rough surfaces [6], combined with multi-channel detection in order to simultaneously extract both the out-of-plane and the in-plane displacements [7]. In this paper, we shortly describe here the design and principle of operation of this ultrasonic receiver and its performances being based on detectors array combined with parallel processing. We will conclude with some applications for Non-Destructive Evaluations.

TWO-COMPONENT TWO-WAVE-MIXING INTERFEROMETER

Principle of Operation

We took advantages on our experience on multi-channel detection and parallel processing [8] to develop a two-wave mixing (TWM) interferometer capable to measuring simultaneously two components of the surface displacement (out-of-plane and horizontal in-plane). We describe in this paper the measurement of two components simultaneously; the same principle can be applied to detect the third component.

In order to achieve high sensitivity, the interferometer must be able to collect as much as possible of the back scattered light and to process efficiently the large number of collected speckles. One well suited interferometer is the adaptive interferometer based on TWM in photorefractive crystal (PRC). Because adaptive interferometers are optimized to collect many speckles, they are not limited with the single-speckle requirement of “classical” interferometer. Moreover, the in-plane information is carried out by the speckled beams that are scattered away from the specular reflection and an interferometer with a large collecting aperture collects speckle beam corresponding to different angle of incidence. It is thus potentially well suited for in-plane detection.

An important feature of an adaptive interferometer using TWM in PRC is that multiple beams can be independently processed inside the same crystal without cross-talk issue. This feature is used to realize a multiplexed interferometer for simultaneous detection of multiple beams corresponding to the observation at different viewing angles of the same illuminated point. We used an optical layout similar to TWM interferometer [6]. The optical setup (shown in Figure 1-A) was adjusted in order to ensure that the entrance pupil (the collecting optic) is imaged on the detector and the single-element detector was replaced with a linear detector array. Each element of the detector array corresponds to a small area of the entrance pupil and thus corresponds to light backscattered along well defined incidence angles. Processing of the interference signals, as a function of the back-scattered angle, provides simultaneously in-plane and out-of-plane displacements [7]. The multi-detector is a linear-array with 16 elements. The collected light is focused on the linear array using a cylindrical lens. In this configuration, we detect the in-plane component along the orientation of the linear array. The orthogonal in-plane component could be detected by rotating of 90° both the linear detector array and the cylindrical lens.

The light backscattered by the sample may not be uniformly distributed depending on the surface roughness. Thus, each channel must be normalized before calculating the in-plane and out-of-plane. Normalization is achieved using automatic gain controlled (AGC) amplifiers monitoring a low frequency calibration signal generated by an internal mirror mounted on a piezo-electric transducer in the path of the reference beam. After amplitude

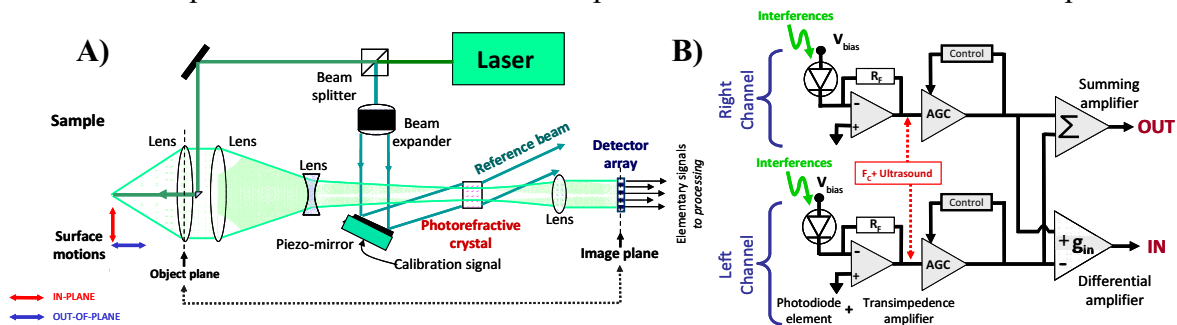


FIGURE 1: A) Optical setup and B) electronic processing for the two components two-wave mixing interferometer for in-plane and out-of-plane displacement detection.

normalization, the signals are processed by pairs having the same incidence angles. For each pair, the two normalized signals are added to generate the elementary out-of-plane component and their subtraction gives the elementary in-plane component [7]. However, the contribution in the final in-plane signal of each elementary in-plane component depends on the angle. A weight is thus applied depending on the angle contribution of the in-plane as show equation (1) for the elementary in-plane and in equation (2) for the out-of-plane components (Figure 1-B).

$$I_i - I_{-i} \propto \left(\frac{4\pi\delta_{IN}}{\lambda} \right) \sin(q_i) \quad (1)$$

$$I_i + I_{-i} \propto \left(\frac{4\pi\delta_{OUT}}{\lambda} \right) \cos(q_i) \quad (2)$$

I_i is the intensity on one photodetector corresponding to the angle q_i of detection and I_{-i} its symmetric. δ_{IN} and δ_{OUT} are respectively the in-plane and out-of-plane displacement.

Performances and Limitations

The main advantage of such a system is its ability to measure simultaneously in-plane and out-of-plane displacement at high frequencies with high sensitivity. TW M in photorefractive crystal does not have an upper frequency limit. The upper frequency limit is given by the detector electronic: 20 MHz for this prototype. The following paragraph describes how the sensitivity of such an interferometer is measured and what performances are achieved.

A critical receiver parameter is the surface displacement sensitivity or minimum detectable displacement called the Noise-Equivalent Surface Displacement (NESD). The NESD is the RMS surface displacement amplitude that can be detected for a signal-to-noise of unity and normalized to 1 W incident power and 1 Hz bandwidth. The units of NESD are $\text{nm} \cdot (\text{W}/\text{Hz})^{1/2}$. An example of noise spectrum measured with the proposed two-component interferometer and on a rough aluminum sample is shown Figure 2. From this noise measurements, we calculate a NESD, for frequency above 1 MHz, of better than $2 \times 10^{-7} \text{ nm} \cdot (\text{W}/\text{Hz})^{1/2}$ for out-of-plane displacement and $11 \times 10^{-7} \text{ nm} \cdot (\text{W}/\text{Hz})^{1/2}$ for the in-plane displacement. Using a 200mW laser, the interferometer collects about 2mW or the detector array.

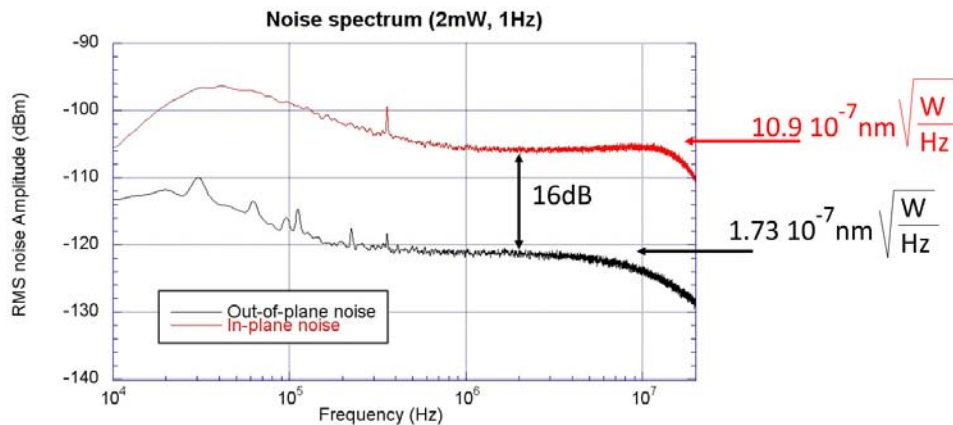


FIGURE 2: Noise spectrum for the calibrated in-plane and out-of-plane outputs achieved with the two-component two-wave-mixing interferometer.

For the in-plane displacement, the sensitivity strongly depends on the spatial distribution of the backscattered light. Optimal conditions are achieved when uniform scattering occurs. The example of NESD measured in Figure 2 corresponds to near-optimal conditions. If the light scattering is not uniform, the noise level of the weakest signals will be amplified through the normalization process, resulting into a higher noise level for the in-plane output. In addition, the in-plane accuracy is given by the numbers of elementary detectors (16 photodiodes for that setup). Increasing the number of element improves the in-plane accuracy, but it also puts more stringent requirements on the detector electronic. Indeed, increasing the number of detector element leads to reduced amount of light per detector element and thus requiring that the detector electronic exhibits lower noise level in order to maintain shot-noise limit detection.

Another main source of noise in such a system comes from the laser. At low frequency the laser intensity noise (LIN) is higher than the shot-noise limit. The noise spectrum on Figure 2 is obtained by implementing in the system a LIN reduction circuit [9] designed to reduce common intensity noise at frequencies below 10 MHz. A 30dB reduction was achieved for low frequency under 1MHz. This reduction feature is needed for the out-of-plane component. Indeed, the in-plane displacement is obtained by subtracting the signal detected by two elementary photodetectors, and thus, the laser intensity noise is naturally rejected due to the differential process of in-plane detection.

The response time of the TWM in $\text{Bi}_{12}\text{SiO}_{20}$ (BSO) permits to compensate the slow phase change (low frequency acoustic vibration for example) of the signal beam but not the small and fast phase change corresponding to the ultrasonic signal (high frequencies). The upper frequency limit of the TWM receiver's bandwidth is thus only limited by the electronic of the detection. However, for measurement on thin samples, background vibrations can easily be picked-up by the thin sample (resonance of a membrane), leading to small ultrasonic signal "jumping" up and down, and if of too large amplitude it could lead to reduction in the system performance as PRC could not compensate fast enough. In order to improve the response time of the receiver, an internal stabilization loop is implemented in the receiver using the piezo-electric transducer in the path of reference beam. Figure 3 shows the response to a negative step without and with the stabilization loop.

With the compensation, the response time is highly improved, with only about $100\mu\text{s}$ to recover from a 66.5nm displacement step when the photorefractive two-wave mixing effect exhibits a "natural" response time of $\tau \sim 3\text{ms}$ to 5ms . Nevertheless, the stabilization loop can only compensate phase vibration. If the vibration is such as the

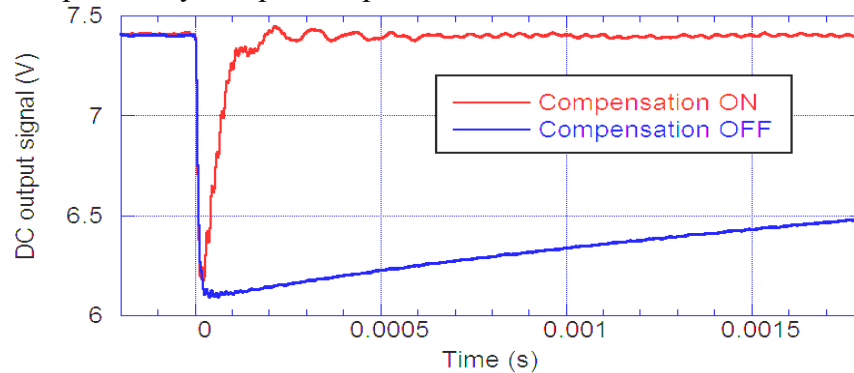


FIGURE 3: Response (measured at DC output) to a negative displacement step of $\lambda/8=66.5\text{nm}$ with and without the compensation feature.

speckle moves too much, then the recovering time is given by the natural response time of the BSO.

Such interferometers are optimized for the measurement of small displacements. We assume the displacement to be small compared to the optical wavelength in order to linearize the sine response of the interferometric detection. With $\lambda=532\text{nm}$, a 30 nm displacement leads to about 5% linearity error.

Finally, in-plane measurement requires detection of light scattered at large incidence angles. This large étendue interferometer has a high numerical aperture and beams detected with the widest angle carry most of the information of the in-plane. The major limitation with high numerical aperture is the corresponding small depth of field. With the implemented system, using a 30 mm stand-off and a 2" aperture, we measured a depth of field of 0.7 mm for in-plane and 2 mm for out-of-plane. An auto-focus feature has been integrated to permit easier alignment and scan.

APPLICATION TO NONDESTRUCTIVE EVALUATIONS

Detection of Through-Transmission Signal Generated by Thermoelastic Laser Pulses

An example of in-plane and out-of-plane detection is show below. Figure 4 describes a through transmission experiment. Generation was achieved in thermoelastic regime with a Nd:YAG pulsed laser. The laser beam was focused along a line with a cylindrical lens. The detection was carried out on the other side of the sample with a bandwidth between 20 kHz and 20 MHz. The sample was a 12.7 mm thick aluminum plate. The laser ultrasonic receiver scanned along a 50 mm line. In a first experiment, we use a sample free of defects (no blind holes). In a second one, two different blind holes (as shown Figure 4) were introduced.

The B-scan results for both in-plane and out-of-plane displacements are shown in Figure 5-A. We can clearly see the direct P-wave (P) and S-wave (S) arrivals at their respective arrival time $2\ \mu\text{s}$ and $4\ \mu\text{s}$, as well as the multiple reflected and reflected/converted waves. As expected, the thermoelastic source generates a stronger S-wave than the P-wave. For these measurements, the calibration coefficient is $100\text{mV}/\text{nm}$ for both in-plane and out-of-plane outputs. After $12\mu\text{s}$, some reflections from the sample edges are also visible on both in-plane and out-of-plane measurement. Moreover, as expected, the in-plane B-scan signal is asymmetrical about the epicenter, whereas the out-of-plane B-scan signal is symmetrical about the epicenter.

Two defects (blind holes as described on Figure 4) were introduced and the measurements were repeated. The result comparing the B-scans, without and with defects,

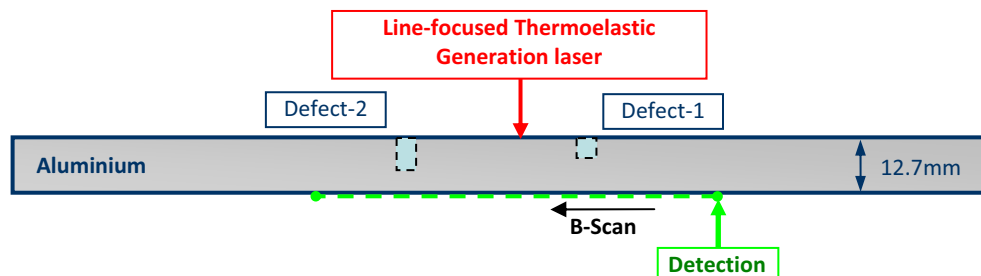


FIGURE 4: Experimental setup for surface wave detection with two-component two-wave mixing ultrasonic receiver. Generation in thermoelastic regime. Detection: B-Scan through transmission.

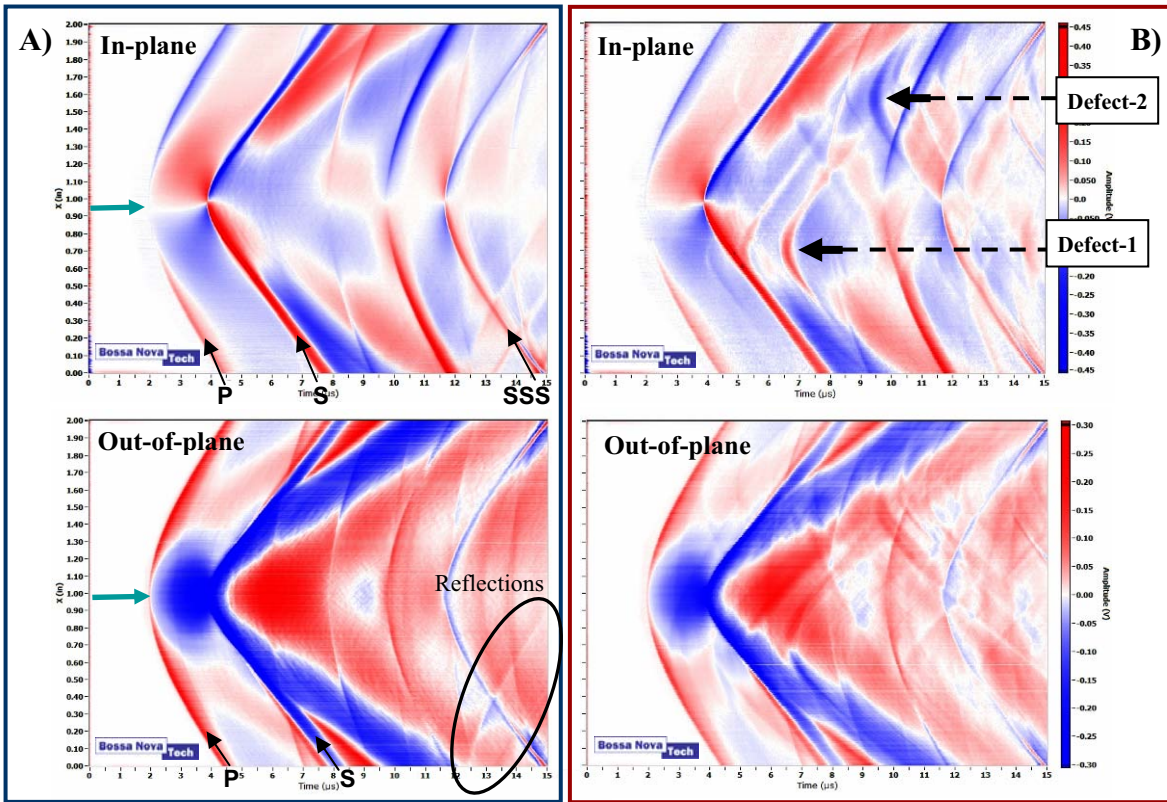


FIGURE 5: B-Scans of through detection setup for in-plane and out-of plane. **A)** No defects; **B)** with defects. The blue arrow on the left shows the epicenter of the generation. Red signal are positive and blue are negative.

is shown Figure 5. Reflection / diffraction from the two defects are visible on both signals, but they are clearly identifiable on the in-plane B-scan.

Lamb Mode Resonance Measurement on Thin Plate

In the next experiment performed the 12.7 mm thick aluminum plate is replaced by a 1 mm thin aluminum sheet. The generation was carried out with a line-focused pulsed laser beam. The measured in-plane direction is along the propagation direction. Figure 6-A shows an example of low-frequency Lamb wave detected with the two-component TWM interferometer after propagation along 50 mm. The detection bandwidth is the same as the previous B-scans. The signals were low-pass filtered with cut-off frequency set at 1MHz, in order to only visualize the lower frequencies for the first set of measurements.

Figure 6-B presents the result of this experiment. The Lamb wave mode A_0 is clearly visible after $16\mu s$ on both graphs. The S_0 mode is clearly present on the in-plane signal, but hardly distinguishable on the out-of-plane. The graph enhances the fact that the symmetrical S_0 mode has a stronger in-plane component which propagates faster than the asymmetrical A_0 mode. Moreover, we can clearly see that the asymmetrical A_0 carries more energy than the S_0 mode. Finally, the A_0 mode presents a phase shift of 90° between the in-plane and out-of-plane component, which justifies its asymmetrical property.

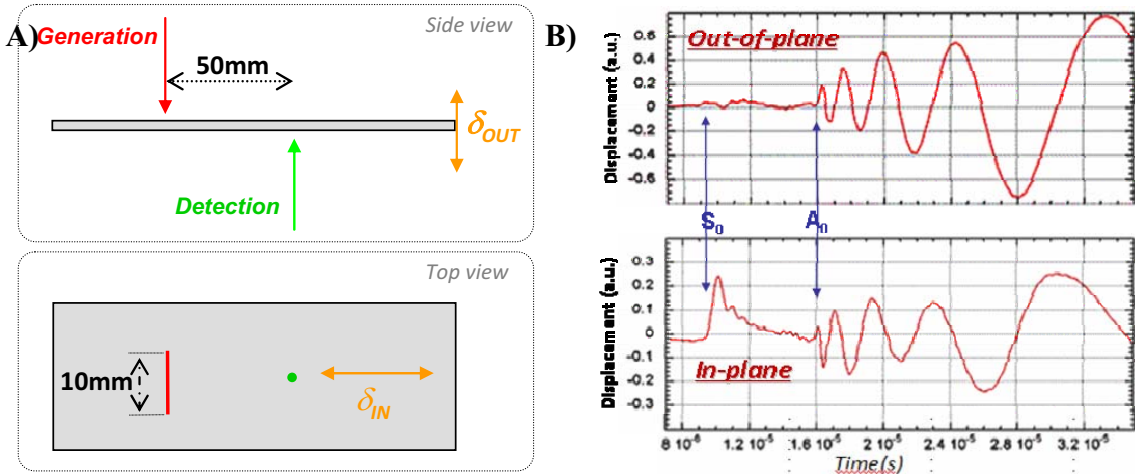


FIGURE 6: A) Experimental setup and B) Low frequency Lamb waves detected in a 1mm thin aluminum sheet, after propagation along 50mm.

A second set of measurements is shown on Figure 7 with detection at the epicenter. Here the data are high-pass filtered, showing only the frequency above 1MHz.

Strong resonances are detected. Some Lamb modes exhibit an anomalous behavior at frequencies where the group velocity vanishes while the phase velocity remains finite. The zero group velocity (ZGV) leads to sharp continuous resonance and ringing effects. Figure 7 shows the fast Fourier transform computed on the first 50 μ s of the signals. The spectrum of the out-of-plane signal (Figure 7-A) and the in-plane signal (Figure 7-B) clearly show the resonance of the S_1 mode and of the A_2 mode as described by Clorennec *et al* [10]. The resonance of the A_2 Lamb mode corresponds to the thickness shear resonance ($F_2 \cdot d = 3 \cdot V_s / 2$), where V_s is the shear wave velocity and d is the thickness.

On the in-plane signal we also see many other resonances at higher frequencies, which were not visible on the out-of-plane displacement.

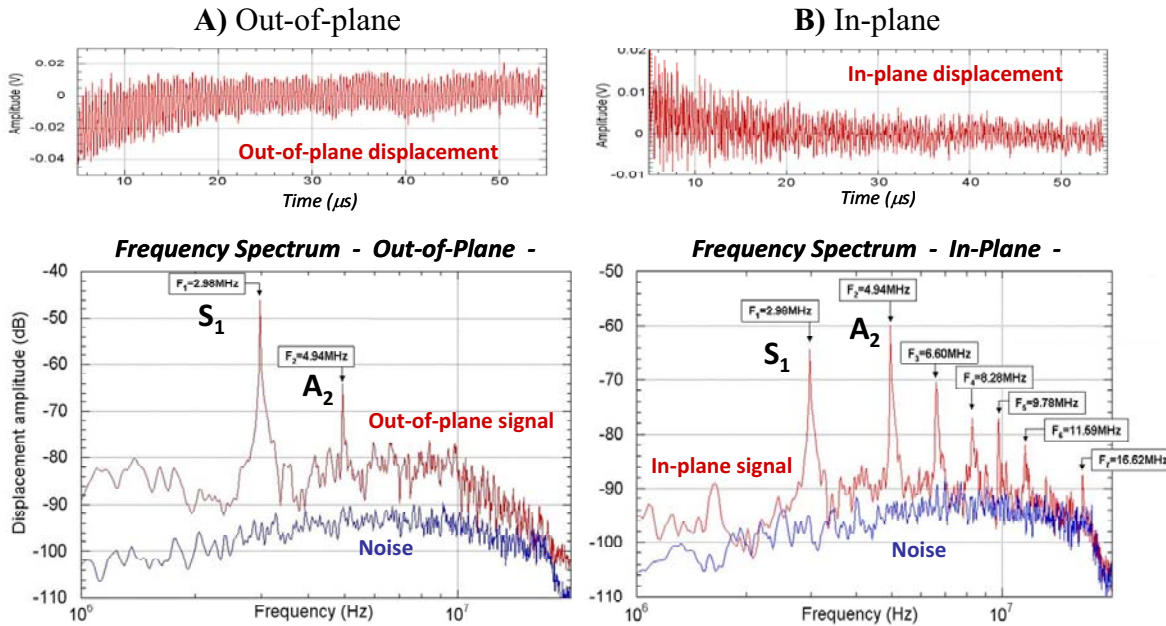


FIGURE 7: Time signal and corresponding Spectrum of the high-frequency Lamb wave, with detection at epicenter. A) out-of-plane displacement and B) In-plane displacement.

CONCLUSION

We have presented a compact optical arrangement which takes advantage of the large optical étendue of TWM interferometer for measuring simultaneously the out-of-plane and in-plane ultrasonic displacements. When measuring only the out-of-plane displacement, this two-component interferometer exhibits the same sensitivity than an optimized single-component interferometer. The in-plane component is obtained without reducing the sensitivity for the out-of-plane component.

The measurement direction of the in-plane component is set by the direction of the linear detector array and the two in-plane components could be extracted simultaneously using either a square array instead of the linear array or an optical arrangement with two linear arrays in a crossed configuration.

REFERENCES

1. Fiedler C. J., in *Review of Progress in QNDE 20*, eds. D. O. Thompson and D. E. Chimenti, Plenum, New York, 2001, p. 308.
2. Monchalain J.-P. et al, in *Review of Progress in QNDE 22*, eds. D. O. Thompson and D. E. Chimenti, Plenum, New York, 2003, p. 264.
3. R.J. Dewhurst, Q. Shan, "Optical remote measurement of ultrasound", *Meas. Sci. Tech.*, 10 (11), pp.R139-R168, 1999.
4. A. Cand, J.-P. Mochalin and X. Jia, "Detection of in-plane and out-of-plane ultrasonic displacements by a two-channel confocal Fabry-Perot interferometer", in *Appl. Phys. Lett.* **64** (4), Jan 1994, ISSN 0003-6951.
5. W. J. Staszewski, B. C. Lee, and R. Traynor, "Fatigue crack detection in metallic structures with Lamb waves and 3D laser vibrometry" *Meas. Sci. Technol.* 18, 727 2007.
6. <http://www.bossanovatech.com/tempo.htm>
7. B. Pouet, N. Lefaudeux, P. Clemenceau, S. Breugnot: "Laser Ultrasonic Inspection Based on In-Plane Detection and Shear Wave Generation" 1st International Symposium on Laser Ultrasonics: Science, Technology and Applications. July 16-18 2008, Montreal, Canada.
8. T. Blum, B. Pouet, S. Breugnot and P. Clémenceau, "Non Destructive Testing Using Multi Channel Random Quadrature Interferometer", *QNDE 2007*, Vol. **27**, Golden, CO.
9. B. Pouet, "Laser Intensity Noise Rejection for Interferometric Apparatus", June 1st 2010, US Patent No: 7,729,881 B2.
10. D. Clorennec, C. Prada, D. Royer and T. Murray, "laser impulse generation and interferometer detection of Zero Group Velocity Lamb mode resonance", *Appl. Phys. Lett.* 89, 2006.